ARTICLES
https://doi.org/10.1038/s41561-020-00660-6
nature geoscience

The role of environmental factors in the long-term evolution of the marine biological pump

Mojtaba Fakhraee[1,2,3]✉, Noah J. Planavsky[1,3] and Christopher T. Reinhard[2,3]

The biological pump—the transfer of atmospheric carbon dioxide to the ocean interior and marine sediments as organic carbon—plays a critical role in regulating the long-term carbon cycle, atmospheric composition and climate. Despite its centrality in the Earth system, the response of the biological pump to biotic innovation and climatic fluctuations through most stages of Earth's history has been largely conjectural. Here we use a mechanistic model of the biological carbon pump to revisit the factors controlling the transfer efficiency of carbon from surface waters to the ocean interior and marine sediments. We demonstrate that a shift from bacterioplankton-dominated to more eukaryote-rich ecosystems is unlikely to have considerably impacted the efficiency of Earth's biological pump. In contrast, the evolution of large zooplankton capable of vertical movement in the water column would have enhanced carbon transfer into the ocean interior. However, the impact of zooplankton on the biological carbon pump is still relatively minor when compared with environmental drivers. In particular, increased ocean temperatures and greater atmospheric oxygen abundance lead to notable decreases in global organic carbon transfer efficiency. Taken together, our results call into question causative links between algal diversification and planetary oxygenation and suggest that climate perturbations in Earth's history have played an important and underappreciated role in driving both carbon sequestration in the ocean interior and Earth surface oxygenation.

The co-evolution of Earth's oceans and the marine biosphere has played a central role in shaping atmospheric chemistry, the evolution of the climate system and long-term planetary habitability. An integral component of this co-evolution is the marine biological carbon pump, in which photosynthesis in sunlit ocean surface waters and subsequent sinking of particulate organic matter transfers atmospheric carbon to the ocean interior and seafloor sediments, thereby shaping ocean chemistry[1,2] and modulating the abundances of CO_2 and O_2 in Earth's atmosphere[3,4]. Observations in the modern oceans indicate that the overall effectiveness of biological carbon pumping is governed by a wide range of physical, chemical and biological factors, including the aggregation and disaggregation of organic-rich 'marine snow' particles, microbial metabolic function, diel vertical migration (DVM), grazing and faecal pellet production by zooplankton and interaction between aggregates and suspended 'ballast' minerals (for example, refs. [3,5,6]). All of these factors have changed considerably over geologic time, potentially driving fundamental changes to global biogeochemical cycles[7–10].

Multiple biotic innovations, in particular the rise of eukaryotic primary producers (algae), the emergence of zooplankton and the onset of widespread mineral ballasting of primary producer biomass, have been proposed to have reshaped the nature of the biological carbon pump over time[8,11,12]. Although unicellular prokaryotic organisms seem to have been the dominant oceanic primary producers for the vast majority of Earth's history[9,10], there was a shift to more eukaryotic (algal) primary producers (and thus larger phytoplankton cell sizes) during the Neoproterozoic era (between 1,000 and 635 million years ago (Ma))[9,13–16,17]. The subsequent radiation of zooplankton grazers sometime near the Precambrian/Cambrian boundary[9,18–20] would have reshaped surface marine ecosystems and introduced the repackaging of organic matter in faecal pellets[21]. The emergence of larger zooplankton in the Palaeozoic era (~540–240 Ma) with the ability to move vertically through the water column, in a process commonly referred to as DVM, could have further enhanced the transfer of carbon into the ocean interior[22,23]. Widespread biomineralization in primary producers emerged later still in Earth's history, with calcareous phytoplankton becoming common roughly 150–100 Ma and siliceous phytoplankton becoming important primary producers in the Cenozoic era (<65 Ma)[10,24,25]. All of these changes could have potentially important impacts on the dynamics of the ocean biological carbon pump, with potentially far-reaching influence on ocean–atmosphere oxygenation, isotopic excursions, major climatic perturbations and the early evolution of complex life[8,26,27]. However, there have been limited systematic comparisons of the relative impacts of biotic, ecological and abiotic environmental factors on structuring major changes to the ocean's biological carbon pump over geologic time.

A mechanistic model of the marine biological carbon pump

In this Article, we present a new mechanistic model of the ocean biological carbon pump and use it to evaluate how the effectiveness of the biological pump has changed throughout Earth's history. At its core, our model couples stochastic particle aggregation and transport with temperature- and oxygen-dependent organic matter remineralization (Fig. 1a). The constitutive elements of the model, aggregates, are clusters of phytoplankton cells (for example, diatoms, large-sized non-skeletal algae, small-sized picoplankton or zooplankton with various feeding strategies and ecologies) and terrigenous dust particles. In the uppermost layer of the ocean, we probabilistically 'seed' a stock of primary particles based on assumed primary productivity of picoplankton and algal biomass, algal calcite flux and surface dust flux. These particles then sink from the surface ocean and interact in the ocean interior through aggregation/disaggregation and organic matter respiration.

In the ocean interior, particle aggregation in the model is controlled by particle collision rate and aggregation efficiency

[1]Department of Earth and Planetary Sciences, Yale University, New Haven, CT, USA. [2]School of Earth and Atmospheric Sciences, Georgia Tech, Atlanta, GA, USA. [3]NASA Astrobiology Institute, Alternative Earths Team, Riverside, CA, USA. ✉e-mail: mojtaba.fakhraee@yale.edu

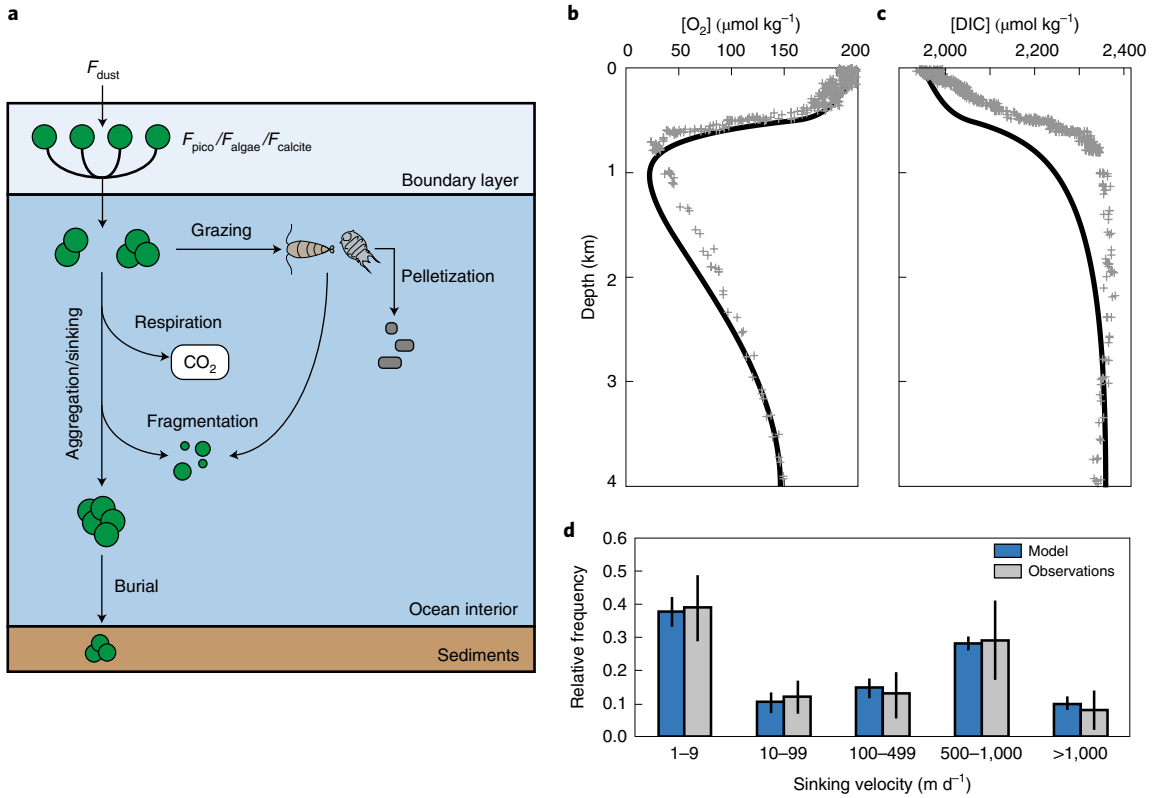

Fig. 1 | Schematic of the mechanistic model of the ocean biological carbon pump discussed in the text. a, The major processes controlling the transfer efficiency of organic carbon in marine sediments (Supplementary Information). F_{dust}, F_{pico}, F_{algae} and $F_{calcite}$ represent imposed relative fluxes of windblown dust, picoplankton, eukaryotic algae, and calcite, respectively, in primary particles. **b**–**d**, Comparison of results from our modern model configuration (black curves) with observational water column data from the North Pacific Ocean[46] (grey crosses) for concentration of dissolved oxygen ($[O_2]$; **b**) and dissolved inorganic carbon ([DIC]; **c**) together with validation of model results against observations of the size–velocity spectrum of marine aggregates in the modern oceans[47,48] (**d**). Error bars in **d** denote one standard deviation.

('stickiness'; compare with ref. [28]). The particle collision rate is in turn controlled by a series of size-dependent processes; very small particles encounter each other by Brownian motion, whereas larger particles meet each other (and smaller particles) through either fluid shear or differential settling (that is, larger particles settle more rapidly and 'sweep up' smaller particles). The model also accounts for the effect of zooplankton on oceanic aggregates and fully parameterizes the impacts of primary production, zooplankton velocity, turbulence and zooplankton faecal pellet size (Supplementary Information). Zooplankton in the model are classed into several groups: small and large zooplankton with and without a central through-going gut (section 4 in the Supplementary Information). To explore the effect of DVM, the model considers both migrating and non-migrating zooplankton (Supplementary Fig. 1). Both small and large zooplankton can either fragment and break down aggregates into several smaller daughter particles or ingest them and produce a wide range of faecal pellet sizes, depending on their prosome length[28]. Rates of zooplankton–aggregate interaction are parameterized to account for both behavioural (for example, active) and physical (for example, turbulent) encounters[29]. Our model thus incorporates aspects from several plankton and zooplankton models developed over the past decade (for example, refs. [28,30]), rather than following a single previously utilized scheme.

Our model is also designed to systematically examine the effects of temperature and oxygen availability on the biological pump. The rate of organic matter degradation in the model is assumed to follow a power-law function (following ref. [31]), which explicitly considers the effect of enhanced organic matter degradation under oxic conditions[32]. To take into account the effect of temperature on the efficiency of the biological carbon pump, we modified the degradation power law in our model by incorporating a temperature dependency factor, Q_{10}, which for most biological systems is somewhere between 1.5 and 2.5 (ref. [33]). Temperature is widely accepted as an important control on the rate of organic matter degradation across a range of ecosystems[34,35,36]. However, the overall impact of temperature relative to other potential controls on carbon transfer in the ocean interior, such as atmospheric oxygen abundance and major changes in the composition of surface marine ecosystems, is poorly known, as is the potential impact of temperature variability on carbon degradation in the power-law organic matter remineralization scheme implemented in our model.

The model implements the particle dynamics and respiratory kinetics in a reaction–transport scheme, which resolves a dissolved oxygen depth profile and oxygen penetration depth (OPD) in the ocean interior (Fig. 1). When forced by modern boundary conditions, the results of our model are consistent with measurements of dissolved oxygen and inorganic carbon from modern marine settings (Fig. 1b,c). Our model also shows the characteristic bimodal sinking rate distribution for marine aggregates observed across a range of modern marine systems (Fig. 1d). Taken together, these observations suggest that our mechanistic model can capture the major factors linking the biological pump to the partitioning of carbon and oxygen in the ocean interior.

To illustrate the major factors controlling the effectiveness of the biological carbon pump in the context of Earth system evolution, we present results from simulations designed to capture the

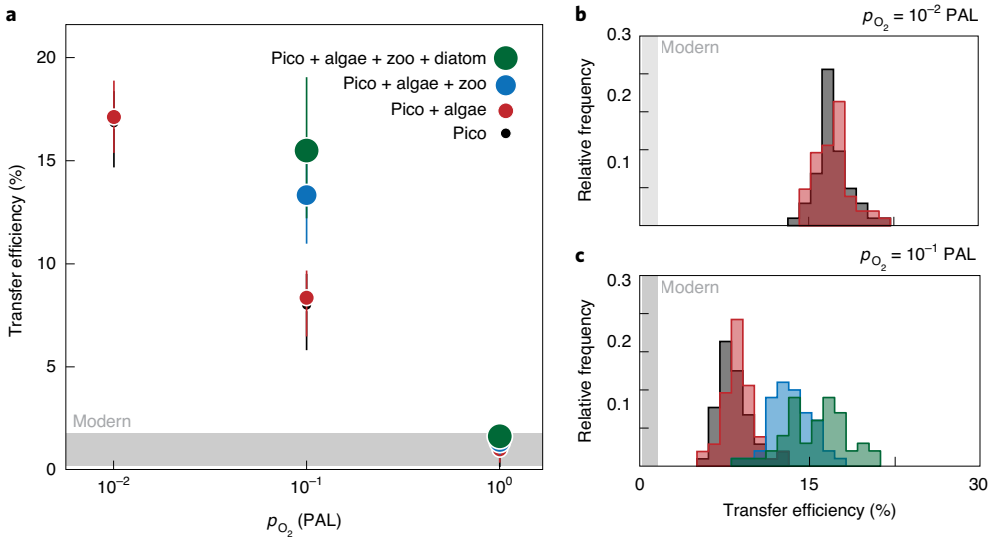

Fig. 2 | The impact of first-order changes to plankton ecology on the ocean biological carbon pump. Values of transfer efficiency are calculated using the oxic and anoxic power laws[32] and without temperature dependency on organic carbon remineralization (Q_{10} = 1). **a**, Net organic carbon transfer efficiencies as a function of atmospheric p_{O_2} relative to PAL and across a range of ecological scenarios: (1) default Precambrian scenario with picoplankton, no algae and high dust flux due to lack of land plants (pico; black); (2) a late Proterozoic scenario, similar to (1) but with a small contribution of algae to ocean productivity (pico + algae; red); (3) an early Phanerozoic scenario, with faecal pellet production by zooplankton and increased contribution of algae (pico + algae + zoo; blue); and (4) a late Phanerozoic scenario with more complex eukaryotic algae (including diatoms) and an attenuated dust flux promoted by the emergence of vascular planets in terrestrial ecosystems (pico + algae + zoo + diatom; green). Error bars show the 90% credible interval from a Monte Carlo analysis of model parameters (Supplementary Information). **b**,**c**, Resampled distributions at two discrete atmospheric p_{O_2} values, with colours corresponding to the scenarios shown in **a**. Modern open-ocean organic carbon transfer efficiencies are shown in all panels by grey shaded boxes[49].

major evolutionary stages of Earth's planktonic marine ecosystems. Specifically, we present idealized scenarios meant to represent: (1) Precambrian time, in which picoplankton are the dominant primary producer and there is a relatively high dust flux to the surface ocean due to a lack of land plants; (2) late Neoproterozoic time, during which eukaryotic algae become important ocean producers; (3) early Phanerozoic time, when increased eukaryotic contributions are combined with robust faecal pellet production by zooplankton; and (4) a modern-like Earth system, in which more complex, mineral-ballasted eukaryotic algae (diatoms and coccoliths) are present along with large DVM-practicing zooplankton, and in which there is an attenuated dust flux as a result of the presence of vascular plants in terrestrial ecosystems. For each scenario, we use a stochastic approach in which we specify atmospheric oxygen as a boundary condition, then sample randomly from uniform priors for all other model parameters and run the model to calculate organic carbon transfer efficiency and OPD in the ocean (Supplementary Table 2). We also explore simulations that more clearly show the isolated effects of individual innovations (for example, biomineralization) and feeding strategies (for example, presence and absence of a through-going gut) (Supplementary Fig. 9).

Biological controls on the ocean's carbon pump

Changes in plankton cell size play only a minor role in the transfer efficiency and the distribution of dissolved oxygen in the oceans (Fig. 2 and Supplementary Figs. 9 and 10). While increases in primary producer cell size and density tied to the increasing importance of eukaryotic algae do result in higher sinking rates in the uppermost water column, there is little difference in overall organic carbon transfer efficiency (Fig. 2a,b). This is due in part to the fact that the formation of marine aggregates is largely independent of the initial cell size of marine primary producers, consistent with experimental results and observations in modern marine settings that suggest lithogenic ballast can effectively create aggregates that sink rapidly through the marine water column[37,38]. At a given atmospheric oxygen level, the transfer efficiencies of the marine carbon pump for scenarios with and without eukaryotic algae largely overlap and the central modes of the simulation ensembles are within ~2%. This difference is clearly not substantial enough to alter oxygen distributions in the ocean interior, as shown by water column OPDs (Supplementary Fig. 10). Our results show that increasing cell size associated with the expansion of eukaryotic algae would not, on its own, promote deeper organic matter remineralization depths and more pervasive ocean oxygenation. Biomineralizing algae similarly have a minor (<5%) effect on efficiency of the biological pump (Supplementary Fig. 9) and OPD (Supplementary Fig. 13).

Our model results also suggest that the radiation of zooplankton lacking the ability to practice DVM during the late Neoproterozoic would have had a limited effect on the efficiency of the carbon pump (Supplementary Fig. 9). This result holds regardless of the dominant zooplankton (for example, with or without a through-going gut; Supplementary Fig. 9). However, the subsequent emergence of DVM by large vertically migrating zooplankton in Palaeozoic seas could have enhanced the flux of particulate organic carbon (POC) into the ocean interior. For example, at an atmospheric partial pressure of oxygen (p_{O_2}) of 10% of the present atmospheric level (PAL), faecal pellet production by zooplankton can increase the overall transfer efficiency of the carbon pump by about 7% (Fig. 2c)[39]. Further, our model predicts that the evolution of DVM in larger zooplankton acts to promote the formation of a pronounced mid-depth oxygen minimum zone (Supplementary Fig. 10). By translocating reactive organic matter from epipelagic into mesopelagic depths, DVM increases oxygen consumption in the ocean interior, which in turn expands the volume of oxygen-poor waters at intermediate depths (Supplementary Fig. 10).

The radiation of swimming animals may have also increased the OPD by promoting mixing in the epipelagic and mesopelagic zones[23]. Although the extent to which swimming animals can alter

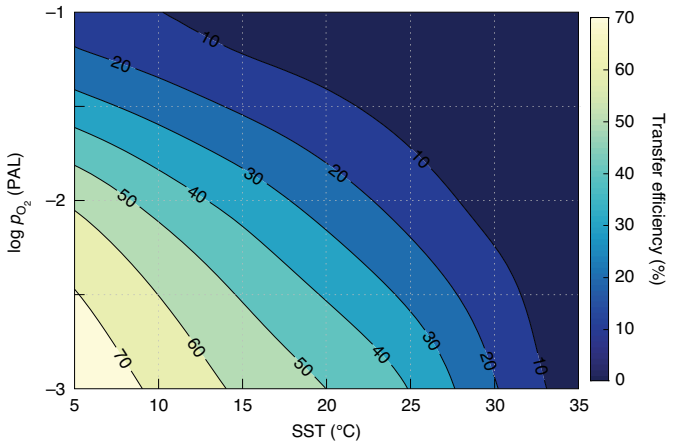

Fig. 3 | The impact of ocean temperature and atmospheric oxygen abundance on the ocean biological carbon pump. Temperatures are reported as sea surface temperature (SST), while atmospheric p_{O_2} is given relative to PAL. Note the log scale for atmospheric p_{O_2}. Organic carbon transfer efficiency (%) is calculated as the fraction of carbon exported from the surface ocean that is delivered to the sediment–water interface.

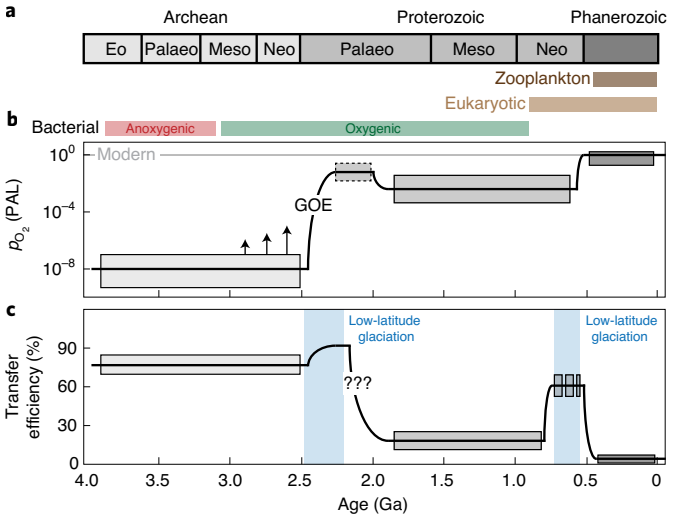

Fig. 4 | The strength of the biological carbon pump through geologic time. **a**–**c**, Changes in ocean ecosystems (**a**), atmospheric oxygen level (**b**) and transfer efficiency of the marine carbon pump (**c**) over time (Ga; billion years ago). We suggest that the strength of the biological carbon pump on geological timescales is mainly controlled by environmental factors such as atmospheric oxygen abundance and shifts in mean climate state. Predominantly anoxic conditions during the Precambrian (>500 Ma) promoted a relatively efficient carbon pump (even if overall productivity was relatively low[50]), with transient increases in transfer efficiency occurring during major climate cooling during low-latitude Snowball Earth glaciations such as those suggested during and after the great oxidation event (GOE) and during the Neoproterozoic era. The grey boxes in **c** show results from our model under evolving atmospheric oxygen levels according to **b**[7], with suggested transient intervals of oxygenation during the late Archaean shown by arrows. The thickness of each box corresponds to uncertainty associated with variability in model input parameters (Supplementary Tables 1 and 2), and the assumed ranges in atmospheric oxygen abundance. Uncertainty in the levels of atmospheric oxygen after the GOE (depicted by the dashed line in **b**) makes the transfer efficiency at this time harder to constrain.

the structure of the physical mixing in the modern ocean is currently debated[40–42] (section 6.2 in the Supplementary Information), we explore the potential effect of increased biogenic mixing on our model results by artificially increasing the turbulent coefficient to mimic increased epipelagic and mesopelagic mixing by swimming organisms (Supplementary Information). A notable increase (for example, a doubling) in the turbulent coefficient does enhance oxygen availability in the ocean, causing an increase in a minimum concentration of dissolved oxygen [O_2] from around 1.5 µM to 6 µM. However, the overall effect of this on the transfer efficiency of the carbon pump is minimal (Supplementary Fig. 3). Nevertheless, our results raise the intriguing possibility[23] that metazoan-induced turbulence may have exerted an equal or more pronounced effect on marine oxygen levels and the transfer efficiency of the biological pump than zooplankton faecal pellet production.

Environmental drivers on the ocean's carbon pump

Environmental factors have a much more pronounced effect on the efficiency of the biological carbon pump and marine oxygen dynamics in our model than biotic innovations. More precisely, in our model, temperature and atmospheric oxygen abundance play far more important roles in structuring transfer efficiency of organic carbon than cell size, mineral ballasting, zooplankton faecal pellet production or DVM (Fig. 3). Mechanistically, elevated temperature leads to a shallower organic matter remineralization depth in the water column, leading to reduced organic matter transfer into the ocean interior and attenuated delivery to seafloor sediments, which should ultimately lead to decreased geological sequestration of organic carbon. This is consistent with measurements in modern deep marine sediments showing accumulation of labile, low-molecular-weight organic carbon at lower temperatures[43], which has been tied to sluggish organic matter degradation kinetics. It is also consistent with observations from modern marine water columns, which show deeper organic matter remineralization depths as water temperature drops[44].

Similarly, decreases in oxygen availability can lead to shallower organic carbon remineralization depths, amplifying the impact of temperature at relatively low atmospheric p_{O_2} (Figs. 2a and 3). Changes in atmospheric oxygen and seawater surface temperature also substantially impact OPD in the ocean. Shifts in either atmospheric oxygen level or temperature over ranges commonly predicted for the past billion years of Earth's history have a far greater impact on the transfer efficiency of the carbon pump and marine oxygen levels than any biologically induced change (Fig. 4 and Supplementary Figs. 9–11).

Our results provide a mechanistic basis for evaluating the relative roles of biotic innovation and environmental change in shaping the ocean's biological carbon pump over time (Fig. 4). In particular, our model broadly predicts a secular decrease in the efficiency of the marine carbon pump, largely as a consequence of increasing atmospheric p_{O_2} against a backdrop of a predominantly bacterial carbon pump. However, a more efficient carbon pump at low p_{O_2} during the Precambrian, as predicted by our model, would not necessarily translate to higher total organic matter content in the geologic record, as the total organic matter content in siliciclastic sedimentary rocks is controlled by not only the efficiency of the marine carbon pump but also the local rate of net primary production (NPP) in the ocean (section 5.2 in the Supplementary Information), which itself is governed by nutrient availability (for example, ref. [45]).

In summary, we present a new mechanistic model of the ocean biological carbon pump designed to interrogate first-order changes to the biotic and environmental factors regulating vertical carbon fluxes in Earth's oceans. Our results strongly suggest that the emergence of larger eukaryotic algae and zooplankton predators would have had only a marginal impact on large-scale carbon and oxygen

fluxes in the ocean interior during the late Proterozoic and early Phanerozoic time. The onset of DVM well after the initial diversification of metazoans would have substantially increased organic carbon export into the ocean interior. However, shifts in global climate and ocean–atmosphere oxygen abundance have probably played a more central role in regulating the strength and efficiency of Earth's biological carbon pump over time than any biotic innovation after the rise of oxygenic photosynthesis. This highlights the first-order role of temperature in controlling the large-scale structure of the ocean biological pump and provides a novel link between planetary redox balance and the climate system on geologic timescales.

Online content

Any methods, additional references, Nature Research reporting summaries, source data, extended data, supplementary information, acknowledgements, peer review information; details of author contributions and competing interests; and statements of data and code availability are available at https://doi.org/10.1038/s41561-020-00660-6.

Received: 24 December 2019; Accepted: 19 October 2020;
Published online: 30 November 2020

References

1. Gwizd, S. J. *Paleoceanography of the Eastern Equatorial Pacific: Insights from a new Carnegie Platform Stratigraphic Record*. MS thesis, Univ. California, Santa Barbara (2015).
2. Boyd, P. W. & Trull, T. W. Understanding the export of biogenic particles in oceanic waters: is there consensus? *Prog. Oceanogr.* **72**, 276–312 (2007).
3. Volk, T. & Hoffert, M. I. in *The Carbon Cycle and Atmospheric CO_2: Natural Variations Archean to Present* Vol. 32 (eds Sundquist, E. T. & Broecker, W. S.) 99–110 (American Geophysical Union, 1985).
4. Ducklow, H. W., Steinberg, D. K. & Buesseler, K. O. Upper ocean carbon export and the biological pump. *Oceanography* **14**, 50–58 (2001).
5. Fowler, S. W. & Knauer, G. A. Role of large particles in the transport of elements and organic compounds through the oceanic water column. *Prog. Oceanogr.* **16**, 147–194 (1986).
6. Alldredge, A. L. & Silver, M. W. Characteristics, dynamics and significance of marine snow. *Prog. Oceanogr*. https://doi.org/10.1016/0079-6611(88)90053-5 (1988).
7. Lyons, T. W., Reinhard, C. T. & Planavsky, N. J. The rise of oxygen in Earth's early ocean and atmosphere. *Nature* **506**, 307–315 (2014).
8. Lenton, T. M., Boyle, R. A., Poulton, S. W., Shields-Zhou, G. A. & Butterfield, N. J. Co-evolution of eukaryotes and ocean oxygenation in the Neoproterozoic era. *Nat. Geosci.* **7**, 257–265 (2014).
9. Butterfield, N. J. Plankton ecology and the Proterozoic–Phanerozoic transition. *Paleobiology* **23**, 247–262 (1997).
10. Knoll, A. H. & Nowak, M. A. The timetable of evolution. *Sci. Adv.* **3**, e1603076 (2017).
11. Butterfield, N. J. Oxygen, animals and oceanic ventilation: an alternative view. *Geobiology* **7**, 1–7 (2009).
12. Bartley, J. K. & Kah, L. C. Marine carbon reservoir, C_{org}–C_{carb} coupling, and the evolution of the Proterozoic carbon cycle. *Geology* **32**, 129–132 (2004).
13. Zhang, S. et al. Sufficient oxygen for animal respiration 1,400 million years ago. *Proc. Natl Acad. Sci. USA* **113**, 1731–1736 (2016).
14. Isson, T. T. et al. Tracking the rise of eukaryotes to ecological dominance with zinc isotopes. *Geobiology* **16**, 341–352 (2018).
15. Love, G. D. et al. Fossil steroids record the appearance of Demospongiae during the Cryogenian period. *Nature* https://doi.org/10.1038/nature07673 (2009).
16. Knoll, A. H. & Sperling, E. A. Oxygen and animals in Earth history. *Proc. Natl Acad. Sci. USA* https://doi.org/10.1073/pnas.1401745111 (2014).
17. Planavsky, N. J. et al. No evidence for high atmospheric oxygen levels 1,400 million years ago. *Proc. Natl Acad. Sci.* **113**, E2550–E2551 (2016).
18. Vannier, J. & Chen, J. Y. The early Cambrian colonization of pelagic niches exemplified by Isoxys (Arthropoda). *Lethaia* **33**, 295–311 (2000).
19. Knoll, A. H., Javaux, E. J., Hewitt, D. & Cohen, P. Eukaryotic organisms in Proterozoic oceans. *Philos. Trans R. Soc. Lond. B* **361**, 1023–1038 (2006).
20. Falkowski, P. G. in *Encyclopedia of Biodiversity* 2nd edn, 552–564 (Elsevier, 2013).
21. Logan, B. E. & Wilkinson, D. B. Fractal geometry of marine snow and other biological aggregates. *Limnol. Oceanogr.* **35**, 130–136 (1990).
22. Berry, W. B. N., Wilde, P. & Quinby-Hunt, M. S. Paleozoic (Cambrian through Devonian) anoxitropic biotopes. *Palaeogeogr. Palaeoclimatol. Palaeoecol.* **74**, 3–13 (1989).
23. Butterfield, N. J. Oxygen, animals and aquatic bioturbation: an updated account. *Geobiology* **16**, 3–16 (2018).
24. Polyakova, Y. I. Late Cenozoic evolution of northern Eurasian marginal seas based on the diatom record. *Polarforschung* **69**, 211–220 (1999).
25. Harwood, D. M., Nikolaev, V. A. & Winter, D. M. Cretaceous records of diatom evolution, radiation, and expansion. *Paleontol. Soc. Pap.* **13**, 33–59 (2007).
26. Lenton, T. M. & Daines, S. J. The effects of marine eukaryote evolution on phosphorus, carbon and oxygen cycling across the Proterozoic–Phanerozoic transition. *Emerg. Top. Life Sci.* https://doi.org/10.1042/ETLS20170156 (2018).
27. Tziperman, E., Halevy, I., Johnston, D. T., Knoll, A. H. & Schrag, D. P. Biologically induced initiation of Neoproterozoic snowball-Earth events. *Proc. Natl Acad. Sci. USA* https://doi.org/10.1073/pnas.1016361108 (2011).
28. Jokulsdottir, T. & Archer, D. A stochastic, Lagrangian model of sinking biogenic aggregates in the ocean (SLAMS 1.0): model formulation, validation and sensitivity. *Geosci. Model Dev.* **9**, 1455–1476 (2016).
29. Dzierzbicka-Głowacka, L. Encounter rates in zooplankton. *Pol. J. Environ. Stud.* **15**, 243–257 (2006).
30. Archibald, K. M., Siegel, D. A. & Doney, S. C. Modeling the impact of zooplankton diel vertical migration on the carbon export flux of the biological pump. *Global Biogeochem. Cycles* **33**, 181–199 (2019).
31. Middelburg, J. J. A simple rate model for organic matter decomposition in marine sediments. *Geochim. Cosmochim. Acta* **53**, 1577–1581 (1989).
32. Katsev, S. & Crowe, S. A. Organic carbon burial efficiencies in sediments: the power law of mineralization revisited. *Geology* **43**, 607–610 (2015).
33. Quinlan, A. V. The thermal sensitivity of Michaelis–Menten kinetics as a function of substrate concentration. *J. Franklin Inst.* **310**, 325–342 (1980).
34. Quinlan, A. V. The thermal sensitivity of generic Michaelis–Menten processes without catalyst denaturation or inhibition. *J. Therm. Biol.* **6**, 103–114 (1981).
35. Segschneider, J. & Bendtsen, J. Temperature-dependent remineralization in a warming ocean increases surface pCO_2 through changes in marine ecosystem composition. *Global Biogeochem. Cycles* **27**, 1214–1225 (2013).
36. John, E. H., Wilson, J. D., Pearson, P. N. & Ridgwell, A. Temperature-dependent remineralization and carbon cycling in the warm Eocene oceans. *Palaeogeogr. Palaeoclimatol. Palaeoecol.* **413**, 158–166 (2014).
37. Iversen, M. H., Ploug, H. & Wegener, A. Ballast minerals and the sinking carbon flux in the ocean: carbon-specific respiration rates and sinking velocity of marine snow aggregates. *Biogeosciences* **7**, 2613–2624 (2010).
38. Klaas, C. & Archer, D. E. Association of sinking organic matter with various types of mineral ballast in the deep sea: implications for the rain ratio. *Global Biogeochem. Cycles* **16**, 1116 (2002).
39. Bianchi, D., Stock, C., Galbraith, E. D. & Sarmiento, J. L. Diel vertical migration: ecological controls and impacts on the biological pump in a one-dimensional ocean model. *Global Biogeochem. Cycles* **27**, 478–491 (2013).
40. Kunze, E. Biologically generated mixing in the ocean. *Annu. Rev. Mar. Sci.* **11**, 215–226 (2019).
41. Katija, K. Biogenic inputs to ocean mixing. *J. Exp. Biol.* **215**, 1040–1049 (2012).
42. Kunze, E. Fluid mixing by swimming organisms in the low-Reynolds-number limit. *J. Mar. Res.* **69**, 591–601 (2011).
43. Arnosti, C., Jørgensen, B. B., Sagemann, J. & Thamdrup, B. Temperature dependence of microbial degradation of organic matter in marine sediments: polysaccharide hydrolysis, oxygen consumption, and sulfate reduction. *Mar. Ecol. Prog. Ser.* **165**, 59–70 (1998).
44. Marsay, C. M. et al. Attenuation of sinking particulate organic carbon flux through the mesopelagic ocean. *Proc. Natl Acad. Sci. USA* **112**, 1089–1094 (2015).
45. Laakso, T. A. & Schrag, D. P. A small marine biosphere in the Proterozoic. *Geobiology* **17**, 161–171 (2019).
46. Dore, J. E., Lukas, R., Sadler, D. W., Church, M. J. & Karl, D. M. Physical and biogeochemical modulation of ocean acidification in the central North Pacific. *Proc. Natl Acad. Sci. USA* **106**, 12235–12240 (2009).
47. McDonnell, A. M. P. & Buesseler, K. O. Variability in the average sinking velocity of marine particles. *Limnol. Oceanogr.* **55**, 2085–2096 (2010).
48. Alonso-Gonz lez, I. J. et al. Role of slowly settling particles in the ocean carbon cycle. *Geophys. Res. Lett.* **37**, L13608 (2010).
49. Dunne, J. P., Sarmiento, J. L. & Gnanadesikan, A. A synthesis of global particle export from the surface ocean and cycling through the ocean interior and on the seafloor. *Global Biogeochem. Cycles* **21**, GB4006 (2007).
50. Canfield, D. E., Rosing, M. T. & Bjerrum, C. Early anaerobic metabolisms. *Philos. Trans R. Soc. Lond. B* **361**, 1819–1834 (2006).

Methods

A stochastic model for sinking rates of marine aggregates. The constitutive elements of the model are marine snow aggregates. They are clusters of primary particles, a combination of phytoplankton cells (for example, coccolithophorids, diatoms and picoplankton) and terrigenous dust particles. The model considers the impacts of primary producer cell size, faecal pellet and particle fragmentation by zooplankton, aggregation, temperature, dust flux, biomineralization, ballasting by mineral phases (for example, carbonates), oxygen and the fractal geometry (porosity) of the aggregates on organic matter degradation and sinking rates. To account for spatial heterogeneity, the model calculates the sinking rates of a large number of aggregates in a two-dimensional (1,000 × 1,000) grid at each depth. Dividing the ocean into 1,000 depth intervals results in 10^9 potential aggregates, allowing for extensive three-dimensional heterogeneity. The type of phytoplankton (or terrigenous material) in each aggregate is chosen by a probability value calculated for each type of primary particle based on the ratio of their flux values to total flux. This probability is translated into a density matrix in which the frequency of density values for each primary particle is determined. The model also includes a fully parameterized aggregation process for particles using a stickiness parameter and the rate of collision of each pair of particles. The number of particles at each depth is determined by the average probability of aggregation at each depth. The probability of aggregation between a single *i* aggregate and *j*-type aggregates ($P_{i,j}$) is defined as:

$$P_{i,j} = \gamma(z) \times \frac{\beta(i,j)}{\beta_{\mathrm{ref}}} \times \frac{F_{\mathrm{NPP}}(z)}{F_{\mathrm{NPP}_{\mathrm{ref}}}} \times \frac{F_{\mathrm{dust}}(z)}{F_{\mathrm{dust}_{\mathrm{ref}}}} \quad (1)$$

where γ is the stickiness parameter that varies with depth, β is the rate of collision between aggregates *i* and *j*, F_{NPP} and F_{dust} are the fluxes of NPP and dust, and β_{ref}, $F_{\mathrm{NPP}_{\mathrm{ref}}}$ and $F_{\mathrm{dust}_{\mathrm{ref}}}$ are the reference values for collision rate, flux of NPP and dust flux, respectively. The last two parameters in the expression for probability of aggregation ($\frac{F_{\mathrm{NPP}}(z)}{F_{\mathrm{NPP}_{\mathrm{ref}}}}, \frac{F_{\mathrm{dust}}(z)}{F_{\mathrm{dust}_{\mathrm{ref}}}}$) represent higher probability of collision between aggregates at higher fluxes of particles from primary production and dust. The stickiness parameter, γ, is defined to decrease with depth, similar to the rate of organic matter degradation[51]. This assumption is based on observations in modern marine systems, where the main 'glue' that holds marine snow together in the water column is thought to be an organic compound: transparent exopolymer particles, a mucus-like polysaccharide material exuded by phytoplankton and bacteria[52,53]. It has been suggested that production of these compounds is highest under conditions of nutrient limitation during the senescent phase of phytoplankton blooms[54,55].

The rate of collision, β, between two particles is a result of three mechanisms: very small particles mostly encounter each other by Brownian motion, whereas large particles meet each other due to fluid shear and differential settling (that is, the larger particles settle faster, sweeping up the smaller ones). In this model, similar to previous models[28], the coagulation kernel β is calculated as a sum of the three mechanisms. Averaged probability of aggregation at each depth is then used to determine what portion of particles would be in aggregates in the following depth. For instance, at the very top of the domain, where there is no aggregation, each type of primary particle (for example, picoplankton, dust, and so on) is evaluated for aggregation. The average probability of aggregation at that depth is calculated and used to determine what percentage of particles in the following depth will be incorporated within an aggregate.

Using the probability of aggregation, physical parameters for each aggregate such as radius, porosity, volume and density can be calculated. Aggregate sinking rates are calculated using Stokes' law[56]:

$$u = \sqrt{\frac{8 r_{\mathrm{a}} (\rho_{\mathrm{a}} - \rho_{\mathrm{sw}}) g}{3 \rho_{\mathrm{sw}} f(\mathrm{Re})}} \quad (2)$$

where *g* is the gravity of Earth, ρ_{a} is the density of the material in each aggregate and ρ_{sw} is the density of seawater. For low Reynolds numbers (Re) where viscous forces are dominant

$$f(\mathrm{Re}) = \frac{24}{\mathrm{Re}} \quad \text{and} \quad \mathrm{Re} = \frac{2 r_{\mathrm{a}} u}{\nu},$$

where ν is the kinematic viscosity, *u* is the sinking rate of the aggregate and r_{a} is the aggregate radius. For large Reynolds numbers where turbulence starts to play a role, the drag coefficient is calculated using Whites' approximation:

$$f(\mathrm{Re}) = \frac{24}{\mathrm{Re}} + \frac{6}{(1 + \sqrt{\mathrm{Re}})} + 0.4, \quad (3)$$

which is valid for $\mathrm{Re} < 2 \times 10^4$.

Zooplankton in the model are grouped into small and large zooplankton based on their prosome length and their corresponding behaviour (Supplementary Fig. 1). Small zooplankton in the model interact with oceanic aggregates and can either fragment aggregates and result in smaller-sized aggregates or ingest them and produce a range of faecal pellet sizes, consistent with their corresponding prosome length. Observation in the modern ocean shows an important role of particle disaggregation in POC flux attenuation in the ocean mesopelagic zone[57]. Specifically, evidence of slow sinking oceanic aggregates in the modern deep ocean suggest an important role of disaggregation/fragmentation of the oceanic aggregates in marine biological pump. It has been suggested that fragmentation is mainly caused by turbulent flow in the ocean. However, experimental studies on oceanic aggregates show that larger stresses in excess of those due to turbulent shear in the ocean are needed to break the aggregates, suggesting that fragmentation caused by biological shear is the main control on aggregate fragmentation in the ocean[58]. This is also consistent with the observed decrease in the average size of oceanic aggregates when the zooplankton *Euphausia Pacifica* were abundant[59]. While the degree to which zooplankton influence the physical characteristics of oceanic aggregates is not fully understood, experimental and modelling studies do confirm that interaction between zooplankton and marine particles occurs and can lead to aggregate destruction. However, aggregate destruction is restricted to clades of common zooplankton such as copepods. Other reasonably common types of zooplankton, such as salps, are predicted to induce minimal fragmentation[60].

Large zooplankton are further classed into non-migrating and migrating zooplankton. The migrating zooplankton are representative of zooplankton communities that are able to vertically migrate into the ocean twilight zone during the day and night, a process commonly known as DVM, with consequent impact on POC flux and carbon transfer to depths. Generally, DVM is movement of zooplankton to the twilight zone during the day and swimming back to shallow waters during the night. There are a number of environmental factors suggested to impact DVM including water clarity, oxygen availability, seawater surface temperature, turbulence and predator–prey interactions[61,62]. Modern observations indicate that DVM accounts for between 10 and 50% of the total vertical flux of carbon from shallow waters, suggesting an important role of DVM in transferring fixed carbon into the mesopelagic zone[63].

In the model, we first evaluate the possibility of encounters between oceanic aggregates and zooplankton and then, depending on the zooplankton class, the aggregates can be fragmented (disaggregated) or ingested and a range of faecal pellets produced. The calculated POC flux is then corrected to account for the effect of DVM.

Rate of organic carbon degradation. The model calculates average velocity of sinking aggregates at each depth and uses this to find the age of organic particles (t_{age}):

$$t_{\mathrm{age}} = \frac{z_i}{u_{i,\,\mathrm{average}}}, \quad (4)$$

where z_i is corresponding depth (m) and $u_{i,\,\mathrm{average}}$ is the average velocity of aggregates at depth *i* (m d^{-1}). The rate of organic matter degradation in the model (*R*) is assumed to follow a power-law function ($R = -bt^{-a}C$), as suggested by Middelburg[31]. In this expression, *C* is the concentration of organic matter, the constants *a* and *b* define the rate of organic carbon mineralization, and *t* is the age of organic matter as defined in equation (4).This power law has been recently modified to account for the effect of enhanced organic matter degradation under oxic conditions[32]. To investigate the effect of temperature on the efficiency of the carbon pump, we further modified the power law by incorporating a temperature dependency factor, Q_{10}, which for most biological systems is somewhere between 1.5 and 2.5 (for example, refs. [33,34]).

Oceanic oxygen dynamics. To investigate the effect of environmental and biological factors on the OPD in the ocean, we use a one-dimensional steady-state diffusion–advection model. Specifically, we obtain the depth profiles for oxygen and dissolved inorganic carbon (DIC) by resolving the following ordinary differential equation at steady state:

$$0 = \frac{\mathrm{d}}{\mathrm{d}z}\left[K_z \frac{\mathrm{d}C}{\mathrm{d}z} - C(z)v(z)\right] \pm R. \quad (5)$$

Here *z* is depth below the photic zone, *C* is the concentration of the compound of interest, K_z is the turbulent diffusion coefficient, $v(z)$ is the advection velocity, and *R* represents the rate(s) of reaction(s) that consume or produce a given species. The value of the turbulent diffusion is assumed to be relatively high above the chemocline to reflect the highly convective Ekman layer in the upper ocean, linearly decreases to lower values in the thermocline to reflect the high impediment to vertical mixing caused by strong temperature stratification, and then linearly increases to higher values in the deep ocean where the absence of strong temperature gradient permits more effective vertical mixing. The advection coefficient is estimated by dividing a high-latitude deep convection flux (~50 Sv; 1 Sv = 10^6 m^3 s^{-1}) by the lateral (cross-sectional) area of the deep ocean. Due to uncertainty involved with this estimation, the advection term is multiplied by a fitting parameter, α. Values of diffusion coefficients at the surface, thermocline and deep ocean, along with the fitting parameter for advection term α, are obtained through providing a rough fit against the measured DIC and oxygen depth profiles in the modern oceans[46] (Fig. 1).

For oxygen, the consumption rates include the rates of aerobic respiration and iron oxidation if the water column is anoxic. The rate of oxygen consumption by aerobic respiration (R_{resp}) is simulated using the Michaelis–Menten kinetics:

$$R_{resp} = R_C \frac{[O_2]}{K_i + [O_2]}. \quad (6)$$

Here, K_i is the half saturation constant that describes the affinity of enzymes for their substrate and R_C is the carbon mineralization rate, approximated as $R_C = k[OC]$ where the reactivity k is described by the Middelburg power law as a function of carbon age t_{age}: $\log_{10}k = -0.95 \times \log_{10}t_{age} - 0.81$. The age in the model is calculated using equation (4). The organic matter content, [OC], is estimated by dividing the average velocity resulting from the aggregate model by the NPP.

Data availability

We have chosen not to deposit the data at this time but declare that data supporting the findings of this study are available within this article and its Supplementary Information, and all additional data are available from the corresponding author on request.

Code availability

All additional computer codes are available from the corresponding author on request.

References

51. Martin, J. H., Knauer, G. A., Karl, D. M. & Broenkow, W. W. VERTEX: carbon cycling in the northeast Pacific. *Deep Sea Res.* **34**, 267–285 (1987).
52. Kahl, L., Vardi, A. & Schofield, O. Effects of phytoplankton physiology on export flux. *Mar. Ecol. Prog. Ser.* **354**, 3–19 (2008).
53. Dam, H. G. & Drapeau, D. T. Coagulation efficiency, organic-matter glues and the dynamics of particles during a phytoplankton bloom in a mesocosm study. *Deep Sea Res. 2* **42**, 111–123 (1995).
54. Passow, U. & Alldredge, A. L. Distribution, size and bacterial colonization of transparent exopolymer particles (TEP) in the ocean. *Mar. Ecol. Prog. Ser.* **113**, 185–198 (1994).
55. Engel, A. The role of transparent exopolymer particles (TEP) in the increase in apparent particle stickiness (α) during the decline of a diatom bloom. *J. Plankton Res.* **22**, 485–497 (2000).
56. Alldredge, A. L. & Gotschalk, C. In situ settling behavior of marine snow. *Limnol. Oceanogr.* **33**, 339–351 (1988).
57. Briggs, N., Dall'Olmo, G. & Claustre, H. Major role of particle fragmentation in regulating biological sequestration of CO_2 by the oceans. *Science* **367**, 791–793 (2020).
58. Alldredge, A. L., Granata, T. C., Gotschalk, C. C. & Dickey, T. D. The physical strength of marine snow and its implications for particle disaggregation in the ocean. *Limnol. Oceanogr.* **35**, 1415–1428 (1990).
59. Dilling, L. & Alldredge, A. L. Fragmentation of marine snow by swimming macrozooplankton: a new process impacting carbon cycling in the sea. *Deep Sea Res. 1* **47**, 1227–1245 (2000).
60. Iversen, M. H. et al. Sinkers or floaters? Contribution from salp pellets to the export flux during a large bloom event in the Southern Ocean. *Deep Sea Res. 2* **138**, 116–125 (2017).
61. Cohen, J. H. & Forward R. B. Jr in *Oceanography and Marine Biology: An Annual Review* Vol. 47 (eds Gibson, R. N. et al.) 77–110 (CRC Press, 2009).
62. Bianchi, D., Galbraith, E. D., Carozza, D. A., Mislan, K. A. S. & Stock, C. A. Intensification of open-ocean oxygen depletion by vertically migrating animals. *Nat. Geosci.* **6**, 545–548 (2013).
63. Bollens, S. M., Rollwagen-Bollens, G., Quenette, J. A. & Bochdansky, A. B. Cascading migrations and implications for vertical fluxes in pelagic ecosystems. *J. Plankton Res.* **33**, 349–355 (2011).

Acknowledgements

C.T.R. and N.J.P. acknowledge funding from the National Aeronautics and Space Administration Astrobiology Institute and the National Science Foundation.

Author contributions

All authors designed the research. M.F. developed the model and performed model simulations and sensitivity analyses. All authors interpreted model results and wrote the paper.

Competing interests

The authors declare no competing interests.

Additional information

Supplementary information is available for this paper at https://doi.org/10.1038/s41561-020-00660-6.

Correspondence and requests for materials should be addressed to M.F.

Peer review information Primary Handling Editor: Rebecca Neely.

Reprints and permissions information is available at www.nature.com/reprints.